NeuroImage 161 (2017) 171–178

Contents lists available at ScienceDirect

NeuroImage

journal homepage: www.elsevier.com/locate/neuroimage

AV-1451 PET imaging of tau pathology in preclinical Alzheimer disease: Defining a summary measure

Shruti Mishra [a], Brian A. Gordon [a,b], Yi Su [a], Jon Christensen [a], Karl Friedrichsen [a], Kelley Jackson [a], Russ Hornbeck [a,b], David A. Balota [b,c], Nigel J. Cairns [b,d,e], John C. Morris [b,d], Beau M. Ances [a,b,d], Tammie L.S. Benzinger [a,b,f,*]

[a] Department of Radiology, Washington University in St. Louis, School of Medicine, 510 S. Kingshighway, MC 8131, Saint Louis, MO 63110, USA
[b] Knight Alzheimer's Disease Research Center, Washington University in St. Louis, School of Medicine, 510 S. Kingshighway, MC 8131, Saint Louis, MO 63110, USA
[c] Department of Psychological and Brain Sciences, Washington University in St. Louis, School of Medicine, 510 S. Kingshighway, MC 8131, Saint Louis, MO 63110, USA
[d] Department of Neurology, Washington University in St. Louis, School of Medicine, 510 S. Kingshighway, MC 8131, Saint Louis, MO 63110, USA
[e] Department of Pathology & Immunology, Washington University in St. Louis, School of Medicine, 510 S. Kingshighway, MC 8131, Saint Louis, MO 63110, USA
[f] Department of Neurological Surgery, Washington University in St. Louis, School of Medicine, 510 S. Kingshighway, MC 8131, Saint Louis, MO 63110, USA

A B S T R A C T

Utilizing [18F]-AV-1451 tau positron emission tomography (PET) as an Alzheimer disease (AD) biomarker will require identification of brain regions that are most important in detecting elevated tau pathology in preclinical AD. Here, we utilized an unsupervised learning, data-driven approach to identify brain regions whose tau PET is most informative in discriminating low and high levels of [18F]-AV-1451 binding. 84 cognitively normal participants who had undergone AV-1451 PET imaging were used in a sparse k-means clustering with resampling analysis to identify the regions most informative in dividing a cognitively normal population into high tau and low tau groups. The highest-weighted FreeSurfer regions of interest (ROIs) separating these groups were the entorhinal cortex, amygdala, lateral occipital cortex, and inferior temporal cortex, and an average SUVR in these four ROIs was used as a summary metric for AV-1451 uptake. We propose an AV-1451 SUVR cut-off of 1.25 to define high tau as described by imaging. This spatial distribution of tau PET is a more widespread pattern than that predicted by pathological staging schemes. Our data-derived metric was validated first in this cognitively normal cohort by correlating with early measures of cognitive dysfunction, and with disease progression as measured by β-amyloid PET imaging. We additionally validated this summary metric in a cohort of 13 Alzheimer disease patients, and showed that this measure correlates with cognitive dysfunction and β-amyloid PET imaging in a diseased population.

1. Introduction

The primary pathologies of Alzheimer disease (AD) are β-amyloid plaques and misfolded hyperphosphorylated tau protein in the form of neurofibrillary tangles (NFTs) (Braak et al., 2006). The amyloid cascade hypothesis proposes that the abnormal accumulation of β-amyloid is an early event that induces a cascade of changes that eventually results in tau pathology (neurofibrillary tangles, neuritic plaques and neuropil threads), synaptic and neuronal loss and, eventually, dementia (Hardy and Higgins, 1992). While increased β-amyloid deposition in the brain can be seen decades prior to symptom onset, both postmortem (Delaère et al., 1989; Duyckaerts et al., 1987; McLean et al., 1999) and *in vivo* (Rowe et al., 2007; Villemagne et al., 2011) studies indicate that cross-sectional β-amyloid burden does not strongly correlate with concurrent neurodegeneration and clinical disease severity. In contrast, studies of tau pathology have found that the density of neurofibrillary tangles (NFTs) strongly correlates with both neurodegeneration and cognitive status (Arriagada et al., 1992; Bierer et al., 1995). The relationship between cognition and tau has increased interest in assessing tau pathology *in vivo* as well as developing anti-tau therapies (Giacobini and Gold, 2013). However until recently, measurement of tau *in vivo* have been limited to cerebrospinal fluid (CSF) measurements.

A number of positron emission tomography (PET) tracers targeting *in vivo* tau fibrils have been developed (Marquié et al., 2015; Okamura et al., 2014; Villemagne and Okamura, 2016). Early reports have shown a relationship between increased tracer uptake and worsening cognitive status (Brier et al., 2016; Chien et al., 2013; Day et al., 2017; Gordon et al., 2016; Johnson et al., 2015; Schöll et al., 2016; Wang et al., 2016) Unlike β-amyloid, that has a relatively diffuse deposition in the brain, tau pathology in the context of AD has a stereotypical pattern of propagation, most prominently characterized in early neuropathological work by Braak and colleagues (Braak and Braak, 1991). Tangles are present

* Corresponding author. Washington University in Saint Louis, School of Medicine, 510 S. Kingshighway, MC 8131, Saint Louis, MO 63110, USA.
E-mail address: benzingert@wustl.edu (T.L.S. Benzinger).

http://dx.doi.org/10.1016/j.neuroimage.2017.07.050
Received 14 February 2017; Received in revised form 9 June 2017; Accepted 24 July 2017
Available online 26 July 2017

primarily in the transentorhinal cortex in early stages (Braak 1–2), then progress to the entorhinal cortex, hippocampus and rest of the medial temporal lobe cortex (Braak 3–4) and finally throughout the neocortex (Braak 5–6) (Braak et al., 2006).

The utility of using tau PET as an imaging biomarker for staging preclinical AD individuals will depend on defining a clinically relevant summary measure as well as a cut-off for positivity, similar to cut-offs for β-amyloid PET imaging. Early attempts to define summary measures have forced the tracer into approximations of pathological staging (Schöll et al., 2016; Schwarz et al., 2016). Neuropathological studies sample a finite subset of regions and consider whether any pathology is present in a binary manner. PET quantifies the amount of pathology present in tissue and can continuously sample the whole-brain. Further, the spatial resolution of PET, local properties of the tissue, and potential off-target binding of the tracer may increase or decrease the sensitivity of a given structure to tau PET relative to neuropathological staining. These methodological differences may cause pathologically-derived summary measures of tau PET to be a misrepresentation of the most informative brain regions. Initial reports have suggested this with demonstration of more widespread cortical AV-1451 uptake than initially predicted by Braak & Braak staging (Brier et al., 2016; Gordon et al., 2016; Johnson et al., 2009).

Approximately one-third of cognitively normal older individuals have β-amyloid pathology at autopsy (Morris et al., 1996) and *in vivo* using PET or cerebrospinal fluid assays (Morris et al., 2010). It is currently unknown where in the brain elevated tau as measured by PET is most sensitive in detecting preclinical AD. Here, we utilized a data-derived method to determine the key areas of the brain where AV-1451 binding would be the most informative in detecting early, preclinical levels of tau in cognitively normal older adult populations. Specifically, we utilize a sparse k-means clustering algorithm, previously used to define PiB positivity (Cohen et al., 2013; Villeneuve et al., 2015), to determine the key differentiating areas of the brain where AV-1451 binding is most informative. We propose taking the mean SUVR of these key regions of interest to represent a summary measure of tau retention. We validate the clinical utility of this data-derived measure by relating to early measurers of cognitive dysfunction and disease progression, represented by β-amyloid burden.

2. Materials & methods

2.1. Participants

All participants were drawn from ongoing studies on memory and aging at the Knight Alzheimer's Disease Research Center at Washington University in St. Louis. All cognitively normal (CN) (with Clinical Dementia Rating (Morris, 1993) (CDR = 0)) participants (n = 84) and participants with dementia due to Alzheimer disease (n = 13 CDR > 0, 9 CDR = 0.5, 3 CDR = 1, 1 CDR = 2) who had undergone PET imaging with AV-1451 between 11/2014 and 05/2016 were included in the study. A subset (N = 63/97, episodic memory; N = 52/97, attentional control) completed a neuropsychological battery within 1 year of the AV-1451 scan (mean lag 0.42 yr (sd 0.29 yr)). A subset (N = 80/97) completed a β-amyloid (Aβ) PET scan within 2 years of the AV-1451 scan (mean lag time of 0.36 yrs (sd 0.36 yrs). Demographic information is presented in Table 1. Participants provided informed consent and all procedures were approved by the local IRB and were HIPPA compliant.

2.2. Neuropsychological testing

Two neuropsychological composite measures were computed. The episodic memory composite included the Selective Reminding Test (Grober et al., 1988), Associate Learning from the Wechsler Memory Scale (WMS) (Rubin et al., 1998), and immediate recall of the WMS Logical Memory or WMS-Revised Logical Memory (Wechsler, 1987). The attentional control composite included computerized versions of the Stroop color naming task, the Simon task, and the consonant-vowel/odd-even task-switching paradigm (Aschenbrenner et al., 2015a). In-depth descriptions have been published elsewhere (Aschenbrenner et al., 2015a; Johnson et al., 2009). Tests of memory and attention were selected as both have previously shown to be sensitive to preclinical levels of pathology (Aschenbrenner et al., 2015a, 2015b; Hassenstab et al., 2016; Monsell et al., 2014).

Table 1
Demographics table.

	CDR = 0	CDR>0
N	84	13 (9 CDR 0.5, 3 CDR 1, 1 CDR 2)
Mean Age, yr (SD)	69 (9)	78 (8)
Gender, n male (%)	44 (52%)	6 (46%)
ApoE4, n (%)	24 (29%)	7 (54%)
Amyloid PET status, N Pos from available	18/67	12/13
N underwent episodic memory tests	51/84	12/13
N underwent attentional control tests	46/84	6/13
Mean Lag Time to AV-45 or PiB scan, yr (SD)	0.24 (0.66)	0.44 (0.82)

2.3. MRI imaging

T_1-weighted images were acquired on a Siemens Biograph mMR or TIM Trio 3 T scanner with: repetition time (TR) = 2300 ms, echo time (TE) = 2.95 ms, flip angle (FA) = 9°, 176 slices, in plane resolution 240 × 256, slice thickness = 1.2 mm acquired in sagittal orientation. Images underwent volumetric segmentation using FreeSurfer 5.3 (Fischl et al., 2002) to identify 36 anatomic regions of interest (ROIs), collapsed across left and right hemispheres (all cortical ROIs and the hippocampus and amygdala were included; full list in supplemental section).

2.4. PET imaging

Tau PET imaging was performed using [F-18]- AV-1451. Participants received a single intravenous bolus of between 7.2 and 10.8 mCi of AV-1451. Aβ PET imaging was performed with either florbetapir (AV-45) or Pittsburgh Compound B (PiB). AV-1451 and PiB data were acquired on a Siemens Biograph 40 PET/CT scanner. AV-45 data were acquired on a Biograph mMR scanner. Participants who underwent Aβ PET imaging received either a single intravenous bolus between 6.2 and 19.9 mCi of PiB or a single intravenous bolus between 7.4 and 11.3 mCi of AV-45.

As previously reported PET data were processed using a region of interest approach (Su et al., 2015, 2013). FreeSurfer segmentations using the Desikan atlas were used as the basis of the quantitative analysis to obtain regional SUVR with whole cerebellum (AV-1451) or cerebellar gray (AV-45 and PiB). SUVR data from the left and right hemisphere ROIs were averaged to create bilateral ROIs. Partial-volume correction was performed using a regional spread function (RSF) technique (Rousset et al., 1998; Su et al., 2015). For AV-1451, data from the 80–100 min post-injection window were used for the analysis (Brier et al., 2016; Gordon et al., 2016), and for AV-45 and PiB, data from the 50–70 min and 30–60 post-injection window were used instead, respectively.

Aβ PET positivity from PiB scans was defined as a mean cortical SUVR of 1.42 (Brier et al., 2016; Sutphen et al., 2015), commensurate with a previously defined PiB mean cortical binding potential cut-off of 0.18 (Mintun et al., 2006; Su et al., 2013). An equivalent AV-45 mcSUVR cut-off of 1.22 to define RSF-corrected Aβ PET positivity was defined using linear regression in a cohort of 100 individuals who had both AV-45 and PiB imaging as part of a crossover study.

2.5. Statistics

2.5.1. Sparse K-means w/resampling

We employed the sparse k-means (SKM) method (Witten and

Tibshirani, 2010) to cluster our CN participants into two groups (k = 2) denoting high and low levels of tau. Previous work examining PET β-amyloid deposition using k-means clustering (Cohen et al., 2013; Villeneuve et al., 2015) as well as Gaussian mixture models (Mormino et al., 2014; Villeneuve et al., 2015) indicates that cognitively normal older adult populations can be separated into those with and without elevated levels of Aβ. Similarly we divided our CN population into two populations, one with low level of tau (normal or early preclinical AD) and higher level of tau (later preclinical AD). These participants can be classified as having low and high levels of PET tau, respectively.

Sparse k-means is similar to classical k-means in that the goal is to assign a cluster membership for all participants such that the within-cluster difference is minimized and the between-cluster differences are maximized. Unlike classical k-means, which assumes that all variables are of equal weight, SKM outputs weights of the variables (FreeSurfer ROIs) to determine which most significantly affect the clustering. We combined SKM with a resampling approach previously implemented in the literature (Bi et al., 2011). Briefly, for each of 500 iterations, ROI data (n = 36) for 300 samples (participants) was drawn with replacement from the original data set (84 CN participants) with SKM clustering then applied to each iteration. This process was performed two times. The first time, the most highly weighted ROIs were determined by taking the mean weight of each ROI across the 500 iterations. The second time, an unweighted mean across the four most highly weighted ROIs was computed for each sample. An average of this unweighted mean was taken for all samples (participants) assigned to each cluster, resulting in two mean SUVR values for each iteration, one each for the low and high tau clusters. The midpoint of these two values was taken as the cut-off between the low and high tau clusters. A final cut-off was determined by taking the mean of the midpoints across all 500 iterations. Additionally the proportion of times each of the unique 84 participants was assigned to the high PET tau cluster was calculated.

The number of ROIs selected to be in the summary measure was based on the maximum number of ROIs (n) after which addition of the n+1 next highest weighted ROI did not improve the ability of the summary measure in predicting Aβ PET positivity. Receiver operator characteristic (ROC) curve analyses were completed, iteratively evaluating the area under the curve (AUC) of the top 2, 3, 4, 5, and 6 highest weighted ROIs in predicting Aβ PET positivity. These analyses were completed twice, once within just the CN participants and again with both the CN and AD participants.

2.6. Relationships with Aβ deposition, neuropsychological performance, and clinical status

Partial correlations were calculated in the CN cohort looking at the relationship between tau deposition and neuropsychological composite scores controlling for age and gender. Analyses were undertaken using the unweighted AV-1451 SUVR mean across ROIs from the SKM analysis and across ROIs approximating Braak stages 1–4 constructed with input from a neuropathologist (Fig. 1). For reference, these analyses were also completed in the entire population (CN and AD). Using the derived cut-off, all participants were classified as having low or high tau. In the CN participants who had received both tau PET and AV-45 scans, ANCOVA analyses compared individuals with high and low levels of tau on their AV-45 mcSUVR, controlling for age and gender.

3. Results

3.1. Mean AV-1451 signal in AD

The mean AV-1451 voxel-wise SUVR uptake was averaged within the AD and CN participant cohorts. The difference in mean AV-1451 SUVR between these two groups, at a voxel-wise level was taken to identify the AD-specific tracer uptake seen within our participant cohorts (Fig. 2). Increased AV-1451 retention can be seen in the temporal lobe cortical and subcortical regions as well as retention in the parietal and lateral occipital areas. The spatial pattern of tau deposition seen in our AD individuals is consistent with reports from multiple neuroimaging centers (Gordon et al., 2016; Johnson et al., 2015; Schöll et al., 2016; Schwarz et al., 2016).

3.2. Sparse K-means & resampling weights and cut-offs

The mean weights for each of the ROIs across the first set of 500 simulations are shown in Fig. 3 and Supplemental Table 1. These weights indicate their importance for separating cognitively normal participants into high tau and low tau groups. ROC curve analyses were completed, iteratively evaluating the ability of the top 2, 3, 4, 5, and 6 highest weighted ROIs in predicting Aβ PET positivity. The same results were obtained with both inclusion and exclusion of the cognitively impaired population. When completed within the cognitively normal participants, the AUCs for the summary measures were: 0.676 for top 2 ROIs, 0.691 for the top 3 ROIs, 0.730 for the top 4 ROIs, 0.730 for the top 5 ROIs, 0.730 for the top 6 ROIs. As there was no additional benefit to inclusion of the fifth highest weighted ROI into the summary measure, the four highest weighted ROIs were selected for the summary measure: entorhinal cortex, lateral occipital cortex, inferior temporal cortex, and amygdala. A simple arithmetic mean of these four regions was used as a summary measure for AV-1451 uptake.

During the second set of 500 iterations, a cut-off value and the stability of high tau versus low tau cluster assignments was calculated. The final unweighted SUVR cut-off was found to be 1.25. Because alternative reference regions are still being considered for AV-1451, an identical set of 500 iterations was done with SUVR data that was processed using cerebellar cortex as the reference. Using this reference region, the SUVR cut-off was found to be 1.22. The stability of the high vs. low tau designation was evaluated by looking at the proportion of high tau and low tau classifications for each of the 84 participants in the original data set, as shown in Fig. 4. Of the 84 participants, 18 were classified in the high tau cluster greater than 75% of the time, while 58 of the 84 participants were classified in the low tau cluster greater than 75% of the time. There were 8 participants whose SUVRs were intermediate. The results of the resampling showed that 90% (76 of 84 participants) had

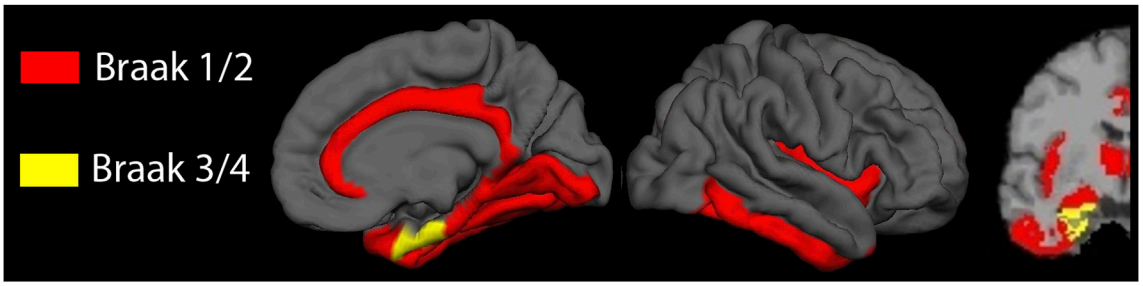

Fig. 1. Pictorial representation of FreeSurfer Regions of Interest assigned to Braak stages 1–4, made in consultation with a neuropathologist.

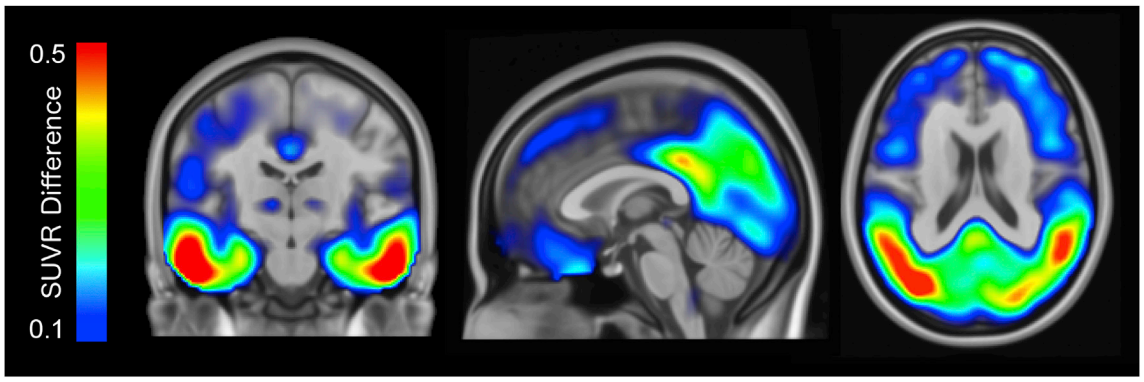

Fig. 2. Axial, coronal, and sagittal planes of the mean difference in AV-1451 SUVR between cognitively normal and Alzheimer diseases individuals.

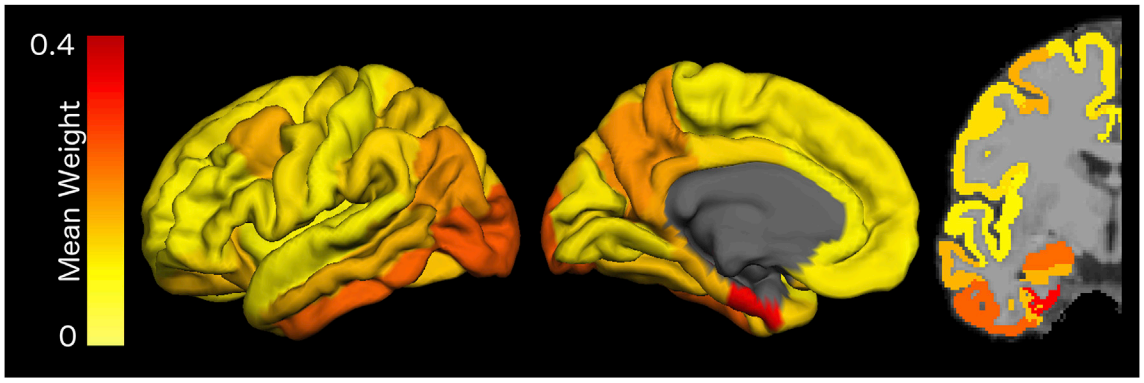

Fig. 3. Mean weights for each of the FreeSurfer Regions of Interest from 500 iterations of the sparse k-means algorithm when clustering cognitively normal participants into k = 2 groups.

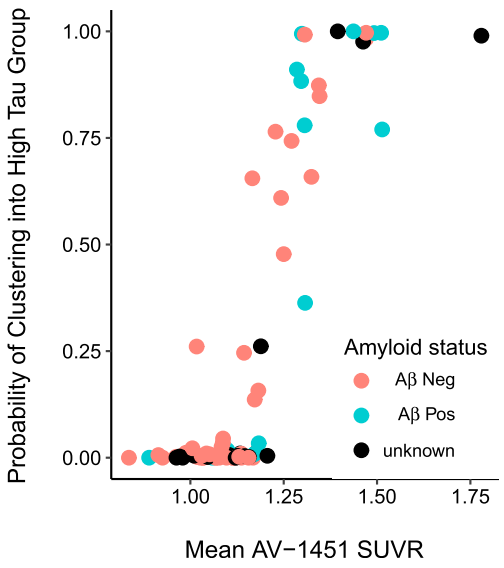

Fig. 4. Proportion of total iterations that each participant was classified in the high tau cluster, as a function of mean AV-1451 SUVR across top four highest-weighted FreeSurfer regions of interest.

consistent cluster membership over 75% of the time. The spread of the mean AV-1451 SUVR in participants classified in the high vs. low tau clusters is depicted in Supplemental Fig. 1.

Utilizing k = 3 did not introduce a new cluster capturing the individuals with inconsistent group membership using k = 2. When utilizing k = 3 the group membership for the high tau cluster was similar, with 16 of the 84 participants being classified into the highest SUVR group greater than 75% of the time. Those that were classified as consistently in the low tau cluster with k = 2 were split between the middle SUVR and lowest SUVR groups, with 25 of the 84 having inconsistent group membership between these groups.

3.3. Relationship of tau PET to neuropsychological measures

The summary measure for AV-1451 uptake as defined above significantly correlated with episodic memory and attentional control in the CN population (Fig. 5). In the CN cohort, when controlling for age and gender, the partial correlation with the PET tau summary measure was r = -0.309 (p = 0.035) for the attentional control composite and r = −0.311 (p = 0.023) for the episodic memory composite. For reference, when including the AD participants, and controlling for age and gender, the relationships between the PET tau summary measure and the neuropsychometric composite scores improved: r = -0.501 (p < 0.001) for attentional control and r = −0.642 (p < 0.001) for episodic memory (not shown in figure).

The utility of the summary measure derived from the SKM clustering was compared with one that was derived by Braak staging. When controlling for age and gender, the partial correlation with the mean SUVR across ROIs in Braak stages 1–4 was r = −0.078 (p = 0.61) for attentional control and r = −0.378 (p = 0.005) for episodic memory (Fig. 6). For reference, when including the AD participants and controlling for age and gender, the relationships between the mean SUVR across ROIs derived from Braak staging and the neuropsychometric composite scores improved: r = −0.456 (p < 0.001) for attentional control and r = −0.658 (p < 0.001) for episodic memory.

3.4. Relationship of tau PET with Aβ PET status

The summary measure for AV-1451 uptake was found to be

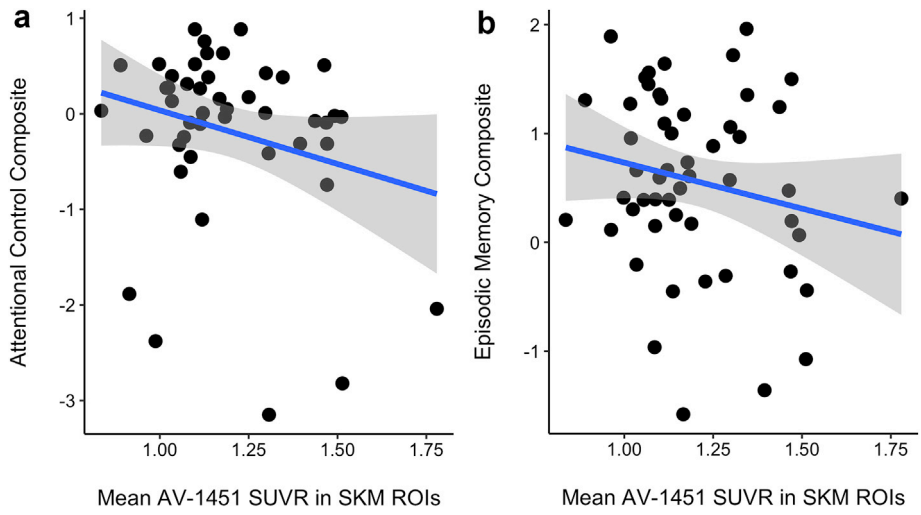

Fig. 5. Relationship between mean AV-1451 SUVR across the top four highest-weighted FreeSurfer regions of interest (SKM ROIs) and A) attentional control composite score and B) episodic memory composite score.

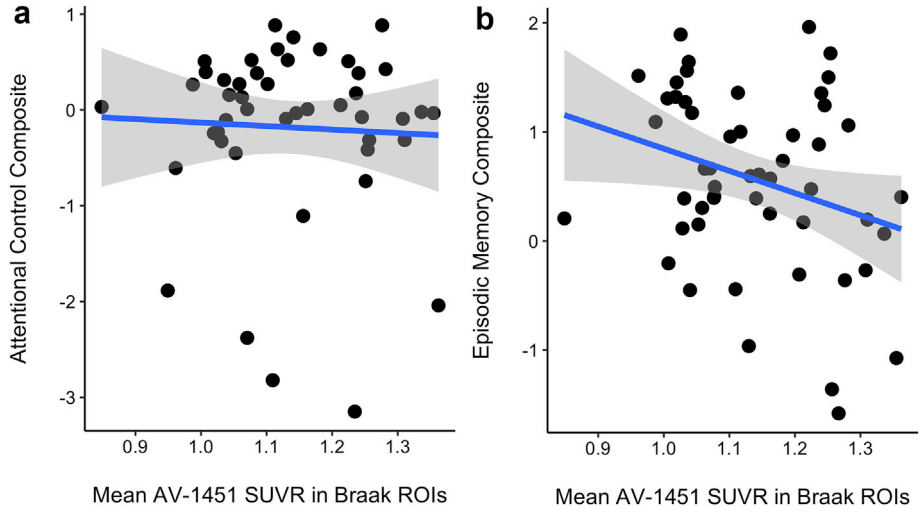

Fig. 6. Relationship between mean AV-1451 SUVR across Braak stages 1–4 FreeSurfer regions of interest (Braak ROIs) and A) attentional control composite score and B) episodic memory composite score.

significantly higher in those cognitively normal participants who were Aβ PET positive in comparison to those who were Aβ PET negative, when controlling for age and gender ($F(1,63) = 12.58$, $p < 0.001$) (Fig. 7A). When classifying each of the cognitively normal participants who also had AV-45 scans as either having high tau or low tau by the cut-off defined above, the participants in the high tau group were found to have significantly higher mcSUVR than those individuals who had low tau after controlling for age and gender ($F(1,54) = 16.90$, $p < 0.001$), as shown in Fig. 7B.

4. Discussion

We sought to define the AV-1451 tau PET regions of interest that are most informative in identifying preclinical levels of tau PET pathology using a data driven method. We found that tau PET in the entorhinal cortex, lateral occipital cortex, inferior temporal cortex and amygdala were most important in differentiating between high tau and low tau individuals, and a partial-volume corrected SUVR cut-off of 1.25 best separated these groups when using the whole cerebellum as a reference region. Moreover, we found that within our CN population tau PET in these data-derived regions correlated with neuropsychological performance and Aβ status.

The introduction of PET Aβ imaging provided a way to detect preclinical AD *in vivo*. Classifying individuals as Aβ+ has become a standardized practice in both research and clinical settings, and has been used as a selection tool to enrich clinical trials (Sperling et al., 2014). Prior work indicates that tau, rather than Aβ pathology is a better predictor of cognition (Arriagada et al., 1992; Bierer et al., 1995). Being able to detect cognitively normal individuals with elevated tau pathology in addition to Aβ will identify those individuals at greatest risk for cognitive decline and potentially further enrich clinical trials beyond using Aβ status alone.

Here, we used a data driven method to arrive at the most clinically relevant regions of interest to be used in a summary metric of tau PET burden. Sparse k-means clustering is a method that has previously been used as an objective method for defining PiB positivity (Cohen et al., 2013; Villeneuve et al., 2015). We made the apriori prediction that our cognitively normal population contains two subpopulations, one that has low levels of tau (either absence or very early stages of AD) and another that has high levels of tau. This prediction was informed by previous evidence that up to one-third of older adult, control patients have pathological evidence of preclinical AD and 27% of our cognitively normal

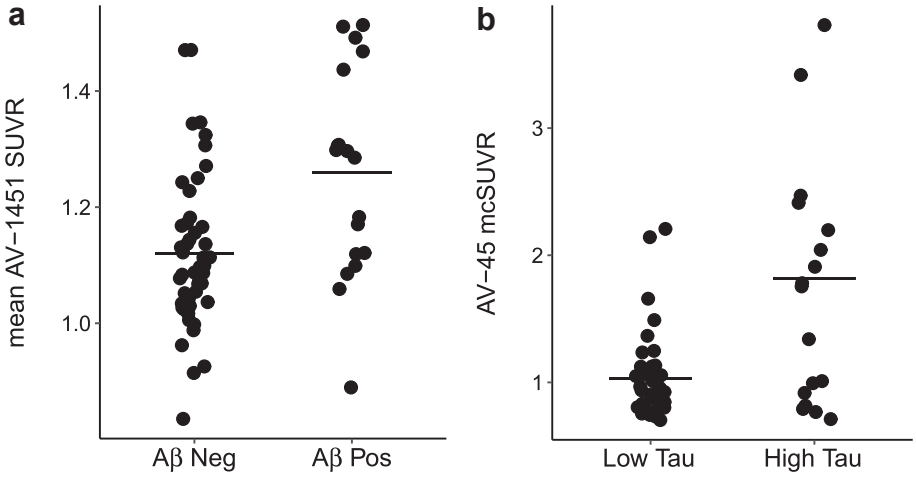

Fig. 7. A) Mean AV-1451 SUVR across the top four highest-weighted FreeSurfer regions of interest in the cognitively normal participants stratified by Aβ positivity and B) Mean AV-45 SUVR in cognitively normal participants, classified as having high tau or low tau based on SUVR cut-off of 1.25.

participant cohort that was Aβ PET positive. The assumption that this population could be represented bimodally was confirmed by the stability of cluster assignment of individuals.

While previous studies have attempted to define cut-offs and summary measures for tau, there have been assumptions that tracer uptake follows the spatial pattern proposed by neuropathological studies (Schöll et al., 2016; Schwarz et al., 2016). While pathology is informative in understanding the stereotypical pattern of spread of neurofibrillary tangles, it is important to acknowledge its limitations. Pathological staging entails testing for the presence of neurofibrillary tangles during finite sampling of specific areas. PET allows for whole-brain quantification of tau burden and in essence reflects the amount or density of tracer uptake in a given area of tissue. The sensitivity of the PET itself is also influenced by the technical properties and constraints (e.g. spatial resolution, off target binding) inherent to the technique. For these reasons the key regions where tau PET will be most informative should not be based solely on the neuropathological as they represent overlapping but not identical properties of the pathology.

The temporal lobe areas of this summary measure are consistent with early tau as proposed by the Braak staging of neurofibrillary tangles in AD (Braak et al., 2006). However, unlike the staging proposed by Braak et al., we found that the lateral occipital cortical region developed PET AV-1451 tau, a region not predicted to have early tau deposition based on pathological staging (Braak et al., 2006). Involvement of the lateral occipital region is seen in prior work with AV-1451 (Brier et al., 2016; Gordon et al., 2016; Johnson et al., 2015; Schöll et al., 2016; Schwarz et al., 2016). Whether this elevation in AV-1451 uptake is secondary to true NFT binding or whether it is secondary to non-NFT binding sites is presently unclear in the field. These results are suggestive that the spatial pattern of AV-1451 uptake in preclinical AD is more widespread than predicted by pathological staging. Whether this is secondary to the methodological constraints of pathological studies, or due to the spatial resolution of PET, the results of this study further corroborate that pathological staging cannot directly be applied to staging tau imaging.

We used an unsupervised learning, k-means clustering approach to determine which regions' levels of tau are most informative for making this cluster assignment. While our methodology produced weights of regions, an unweighted mean of the highest-weighted regions is more easily computed across centers and clinically relevant for future comparisons of tau PET and other biomarkers. We show that this data-derived summary measure has clinical relevance, correlating with performance in neuropsychological testing better than a summary measure derived from Braak neurofibrillary tangle staging in AD. Attentional control is a sensitive measure of early cognitive dysfunction in very mild AD (Perry and Hodges, 1999) as well as preclinical levels of AD pathology (Aschenbrenner et al., 2014). This study provides evidence that tau burden as measured by tau PET may be used to correlate with this biomarker as well as with episodic memory.

We propose an SUVR cut-off of tau positivity of 1.25 using a whole cerebellar reference. As commonly done with other AD biomarkers this cut-off was derived to differentiate between low and high levels of tau within a preclinical population, not as a cut-off between normal and diseased populations. As with other biomarkers, tau PET is a continuous measurement and having low levels of tau PET does not imply the absolute lack of neuronal injury; rather, the cut-off represents levels of injury that are below a clinically meaningful threshold. This preliminary cut-off can be used in the future for staging preclinical AD populations based on National Institute on Aging and Alzheimer's Association guidelines (Sperling et al., 2011).

While the focus of our study was on defining stages in a preclinical population, we also evaluated our summary measure in our participants who either had a clinical diagnosis of Alzheimer disease at the time of the scan or developed it during the course of the study. All but one of these participants was classified in the high tau group. The CDR 0.5 participant who was found to be have low tau had an Aβ PET burden that was below the Aβ cut-off for positivity, suggestive that this participant may be have been misclassified clinically. These results are suggestive that the summary measure will have utility in describing PET tau uptake in diseased populations as well.

There are some limitations of this work. One limitation of our study is the size of our cognitively normal cohort, from which the summary measure and cut-off for positivity was derived. However, there is precedent for establishing cutoffs, in Aβ PET imaging for example, within similarly sized or smaller cognitively normal cohorts (Cohen et al., 2013; Mintun et al., 2006). A second limitation is our use of an unweighted mean from the highest weighted regions of interest in the summary measure of tau. Utilizing an unweighted mean may decrease the sensitivity of the measurement, as it discounts the relative importance of the four ROIs for differentiating between high and low tau cognitively normal participants. Similarly, regions were not weighted by their differential volumes. These choices were made to maximize the generalizability of our approach across clinical and research settings. As more data is accrued by the field and across centers a more nuanced approach may be considered to improve the sensitivity of summary measure even further. In this study, we utilized a sparse k-means method for clustering. We were motivated to use this machine learning algorithm because it is unsupervised and has been used previously to define Aβ PET cutpoints (Cohen et al., 2013; Villeneuve et al., 2015). We recognize that there are alternative methods that could also be used (Jack et al., 2017). Such approaches have their own strengths and limitations, and selecting the

optimal choice is an ongoing discussion within the field. Finally, the most important external validator of this metric will be its ability to track disease progression longitudinally, as a function of clinical status or Aβ biomarkers. This will be a focus for future work, as we begin to acquire longitudinal data with AV-1451 PET.

The work presented here utilizes a data-derived k-means clustering approach to show that tau as measured by AV-1451 PET in the entorhinal cortex, lateral occipital cortex, inferior temporal cortex, and amygdala are most important in detecting elevated tau in preclinical AD. This spatial pattern of AV-1451 uptake is more widespread than predicted by pathological staging, suggestive of more advanced pathology with intact cognitive status than previously thought. Increased tau in these regions correlates with early cognitive impairment, and can differentiate between Aβ positive and negative cognitively normal individuals. Finally, this work proposes an SUVR cut-off of 1.25 across these four regions for differentiating between individuals with high and low levels of PET tau within a cognitively normal population.

Acknowledgements

F18-AV-1451 precursor and technology was supported by Avid Radiopharmaceuticals. F18-AV-45 scans were supported by Avid Radiopharmaceuticals. This work was supported by the National Institutes of Health through the Healthy Aging and Senile Dementia (P01 AG003991), Adult Children's Study (P01 AG026276), and the Alzheimer's Disease Research Center (AG005681), NINDS Center Core for Brain Imaging (P30 NS098577) projects. This research was also supported by the Barnes-Jewish Hospital Foundation.

Appendix A. Supplementary data

Supplementary data related to this article can be found at http://dx.doi.org/10.1016/j.neuroimage.2017.07.050.

References

Arriagada, P.V., Growdon, J.H., Hedleywhyte, E.T., Hyman, B.T., 1992. Neurofibrillary tangles but not senile plaques parallel duration and severity of Alzheimer's disease. Neurology 42, 631–639. http://dx.doi.org/10.1212/WNL.42.3.631.

Aschenbrenner, A.J., Balota, D.A., Fagan, A.M., Duchek, J.M., Benzinger, T.L.S., Morris, J.C., 2015a. Alzheimer disease cerebrospinal fluid biomarkers moderate baseline differences and predict longitudinal change in attentional control and episodic memory composites in the adult children study. J. Int. Neuropsychol. Soc. 21, 573–583. http://dx.doi.org/10.1017/S1355617715000776.

Aschenbrenner, A.J., Balota, D.A., Tse, C.-S., Fagan, A.M., Holtzman, D.M., Benzinger, T.L.S., Morris, J.C., Tse, D.A., Fagan, C.-S., 2014. Alzheimer disease biomarkers, attentional control, and semantic memory retrieval: synergistic and mediational effects of biomarkers on a sensitive cognitive measure in non-demented older adults. Alzheimer Dis. Biomarkers 29, 368–381. http://dx.doi.org/10.1037/neu0000133.

Aschenbrenner, A.J., Balota, D.A., Tse, C.-S., Fagan, A.M., Holtzman, D.M., Benzinger, T.L.S., Morris, J.C., 2015b. Alzheimer disease biomarkers, attentional control and semantic memory retrieval: synergistic and mediational effects of biomarkers on a sensitive cognitive measure. Neuropsychology 29, 368–381. http://dx.doi.org/10.1037/neu0000133.

Bi, W., Tseng, G.C., Weissfeld, L. a, Price, J.C., 2011. Sparse clustering with resampling for subject classification in PET amyloid imaging studies. In: IEEE Nucl. Sci. Symp. Conf. Rec. (1997), vol. 2011, pp. 3108–3111. http://dx.doi.org/10.1109/NSSMIC.2011.6152564.

Bierer, L.M., Hof, P.R., Dushyant, P.P., Carlin, L., Schmeidler, J., Davis, K.L., Perl, D.P., 1995. Neocortical neurofibrillary tangles correlate with dementia severity in Alzheimer's disease. Arch. Neurol. 52, 81–88. http://dx.doi.org/10.1001/archneur.1995.00540250089017.

Braak, H., Alafuzoff, I., Arzberger, T., Kretzschmar, H., Del Tredici, K., 2006. Staging of Alzheimer disease-associated neurofibrillary pathology using paraffin sections and immunocytochemistry. Acta Neuropathol. 112, 389–404. http://dx.doi.org/10.1007/s00401-006-0127-z.

Braak, H., Braak, E., 1991. Neuropathological stageing of Alzheimer-related changes. Acta Neuropathol. 82, 239–259. http://dx.doi.org/10.1007/BF00308809.

Brier, M.R., Gordon, B., Friedrichsen, K., McCarthy, J., Stern, A., Christensen, J., Owen, C., Aldea, P., Su, Y., Hassenstab, J., Cairns, N.J., Holtzman, D.M., Fagan, A.M., Morris, J.C., Benzinger, T.L., Ances, B.M., 2016. Tau and A-beta imaging, CSF measures, and cognition in Alzheimer's disease. Sci. Transl. Med. 8, 1–10. http://dx.doi.org/10.1126/scitranslmed.aaf2362.

Chien, D.T., Bahri, S., Szardenings, A.K., Walsh, J.C., Mu, F., Su, M.-Y., Shankle, W.R., Elizarov, A., Kolb, H.C., 2013. Early clinical PET imaging results with the novel PHF-tau radioligand [F-18]-T807. J. Alzheimers. Dis. 34, 457–468. http://dx.doi.org/10.3233/JAD-122059.

Cohen, A.D., Mowrey, W., Weissfeld, L.A., Aizenstein, H.J., McDade, E., Mountz, J.M., Nebes, R.D., Saxton, J.A., Snitz, B., DeKosky, S., Williamson, J., Lopez, O.L., Price, J.C., Mathis, C.A., Klunk, W.E., 2013. Classification of amyloid-positivity in controls: comparison of visual read and quantitative approaches. Neuroimage 71, 207–215. http://dx.doi.org/10.1016/j.neuroimage.2013.01.015.

Day, G.S., Gordon, B.A., Jackson, K., Christensen, J.J., Rosana Ponisio, M., Su, Y., Ances, B.M., Benzinger, T.L.S., Morris, J.C., 2017. Tau-PET binding distinguishes patients with early-stage posterior cortical atrophy from amnestic Alzheimer disease dementia. Alzheimer Dis. Assoc. Disord. 00, 1–7. http://dx.doi.org/10.1097/WAD.0000000000000196.

Delaère, P., Duyckaerts, C., Brion, J.P., Poulain, V., Hauw, J.J., 1989. Tau, paired helical filaments and amyloid in the neocortex: a morphometric study of 15 cases with graded intellectual status in aging and senile dementia of Alzheimer type. Acta Neuropathol. 77, 645–653. http://dx.doi.org/10.1007/BF00687893.

Duyckaerts, C., Brion, J.-P., Hauw, J.-J., Flament-Durand, J., 1987. Quantitative assessment of the density of neurofibrillary tangles and senile plaques in senile dementia of the Alzheimer type. Comparison of immunocytochemistry with a specific antibody and Bodian's protargol method. Acta Neuropathol. 73, 167–170. http://dx.doi.org/10.1007/BF00693783.

Fischl, B., Salat, D.H., Busa, E., Albert, M., Dieterich, M., Haselgrove, C., van der Kouwe, A., Killiany, R., Kennedy, D., Klaveness, S., Montillo, A., Makris, N., Rosen, B., Dale, A.M., 2002. Whole brain segmentation: neurotechnique automated labeling of neuroanatomical structures in the human brain. Neuron 33, 341–355. http://dx.doi.org/10.1016/S0896-6273(02)00569-X.

Giacobini, E., Gold, G., 2013. Alzheimer disease therapy–moving from amyloid-β to tau. Nat. Rev. Neurol. 9, 677–686. http://dx.doi.org/10.1038/nrneurol.2013.223.

Gordon, B.A., Friedrichsen, K., Brier, M., Blazey, T., Su, Y., Christensen, J., Aldea, P., McConathy, J., Holtzman, D.M., Cairns, N.J., Morris, J.C., Fagan, A.M., Ances, B.M., Benzinger, T.L.S., 2016. The relationship between cerebrospinal fluid markers of Alzheimer pathology and positron emission tomography tau imaging. Brain 139, 2249–2260. http://dx.doi.org/10.1093/brain/aww139.

Grober, E., Buschke, H., Crystal, H., Bang, S., Dresner, R., 1988. Screening for dementia by memory testing. Neurology 38, 900–903. http://dx.doi.org/10.1212/WNL.38.6.900.

Hardy, J.A., Higgins, G.A., 1992. Alzheimer's disease: the amyloid cascade hypothesis. Sci. (80-.) 256, 184–185. http://dx.doi.org/10.1126/science.1566067.

Hassenstab, J., Chasse, R., Grabow, P., Benzinger, T.L.S., Fagan, A.M., Xiong, C., Jasielec, M., Grant, E., Morris, J.C., 2016. Certified normal: Alzheimer's disease biomarkers and normative estimates of cognitive functioning. Neurobiol. Aging 43, 23–33. http://dx.doi.org/10.1016/j.neurobiolaging.2016.03.014.

Jack, C.R., Wiste, H.J., Weigand, S.D., Therneau, T.M., Lowe, V.J., Knopman, D.S., Gunter, J.L., Senjem, M.L., Jones, D.T., Kantarci, K., Machulda, M.M., Mielke, M.M., Roberts, R.O., Vemuri, P., Reyes, D.A., Petersen, R.C., 2017. Defining imaging biomarker cut points for brain aging and Alzheimer's disease. Alzheimer's Dement. 13, 205–216. http://dx.doi.org/10.1016/j.jalz.2016.08.005.

Johnson, D.K., Storandt, M., Morris, J.C., Galvin, J.E., 2009. Longitudinal study of the transition from healthy aging to Alzheimer disease. Arch. Neurol. 66, 1254–1259. http://dx.doi.org/10.1001/archneurol.2009.158.

Johnson, K., Schultz, A., Betensky, R.A., Becker, J.A., Sepulcre, J., Rentz, D., Moromino, E., Chhatwal, J., Ameriglio, R., Papp, K., Marshall, G., Albers, M., Mauro, S., Pepin, L., Alverio, J., Judge, K., Philiossaint, M., Shoup, T., Yokell, D., Dickerson, B., Gomez-Isla, T., Hyman, B., Vasdev, N., Sperling, R., 2015. Tau PET imaging in aging and early Alzheimer's disease. Ann. Neurol. 1–29. http://dx.doi.org/10.1002/ana.24546.

Marquié, M., Normandin, M.D., Vanderburg, C.R., Costantino, I.M., Bien, E.A., Rycyna, L.G., Klunk, W.E., Mathis, C.A., Ikonomovic, M.D., Debnath, M.L., Vasdev, N., Dickerson, B.C., Gomperts, S.N., Growdon, J.H., Johnson, K.A., Frosch, M.P., Hyman, B.T., Gómez-Isla, T., 2015. Validating novel tau positron emission tomography tracer [F-18]-AV-1451 (T807) on postmortem brain tissue. Ann. Neurol. 78, 787–800. http://dx.doi.org/10.1002/ana.24517.

McLean, C.A., Cherny, R.A., Fraser, F.W., Fuller, S.J., Smith, M.J., Bush, A.I., Masters, C.L., 1999. Soluble pool of Abeta amyloid as a determinant of severity of neurodegeneration in Alzheimer's disease. Ann. Neurol. 46, 860–866. http://dx.doi.org/10.1002/1531-8249(199912)46:6<860::AID-ANA8>3.0.CO;2-M.

Mintun, M.A., LaRossa, G.N., Sheline, Y.I., Dence, C.S., Lee, S.Y., Mach, R.H., Klunk, W.E., Mathis, C.A., DeKosky, S.T., Morris, J.C., 2006. [11 C] PIB in a nondemented population Potential antecedent marker of Alzheimer disease. Neurology 67, 446–452. http://dx.doi.org/10.1212/01.wnl.0000228230.26044.a4.

Monsell, S.E., Mock, C., Hassenstab, J., Roe, C.M., Cairns, N.J., Morris, J.C., Kukull, W., 2014. Neuropsychological changes in asymptomatic persons with Alzheimer disease neuropathology. Neurology 83, 434–440. http://dx.doi.org/10.1212/WNL.0000000000000650.

Mormino, E.C., Betensky, R.A., Hedden, T., Schultz, A.P., Ward, A., Huijbers, W., Rentz, D.M., Johnson, K.A., Sperling, R.A., 2014. Amyloid and APOE e 4 interact to influence short-term decline in preclinical Alzheimer disease. Neurology 82, 1760–1767.

Morris, J.C., 1993. The Clinical Dementia Rating (CDR): current version and scoring rules. Neurology 43, 2412–2414. http://dx.doi.org/10.1212/WNL.43.11.2412-a.

Morris, J.C., Roe, C.M., Xiong, C., Fagan, A.M., Goate, A.M., Holtzman, D.M., Mintun, M.A., 2010. APOE predicts amyloid-beta but not tau Alzheimer pathology in cognitively normal aging. Ann. Neurol. 67, 122–131. http://dx.doi.org/10.1002/ana.21843.

Morris, J.C., Storandt, M., McKeel, D.W., Rubin, E.H., Price, J.L., Grant, E.A., Berg, L., 1996. Cerebral amyloid deposition and diffuse plaques in normal aging - evidence for presymptomatic and very mild Alzheimers disease. Neurology 46, 707–719. http://dx.doi.org/10.1212/WNL.46.3.707.

Okamura, N., Harada, R., Furumoto, S., Arai, H., Yanai, K., Kudo, Y., 2014. Tau PET imaging in Alzheimer's disease. Curr. Neurol. Neurosci. Rep. 14, 500. http://dx.doi.org/10.1007/s11910-014-0500-6.

Perry, R.J., Hodges, J.R., 1999. Attention and executive deficits in Alzheimer's disease. A critical review. Brain 122 (3), 383–404. http://dx.doi.org/10.1093/brain/122.3.383.

Rousset, O.G., Ma, Y., Evans, A.C., 1998. Correction for partial volume effects in PET: principle and validation. J. Nucl. Med. 39, 904–911.

Rowe, C.C., Ng, S., Ackermann, U., Gong, S.J., Pike, K., Savage, G., Cowie, T.F., Dickinson, K.L., Maruff, P., Darby, D., Smith, C., Woddward, M., Merory, J., Tochon-Danguay, H., O'Keefe, G., Klunk, W.E., Mathis, C.A., Price, J.C., Masters, C.L., Villemagne, V.L., 2007. Imaging B-Amyloid burden in aging and dementia. Neurology 68, 1718–1725. http://dx.doi.org/10.1212/01.wnl.0000318046.06992.24.

Rubin, E.H., Storandt, M., Miller, J.P., Kinscherf, D.A., Grant, E.A., Morris, J.C., Berg, L., 1998. A prospective study of cognitive function and onset of dementia in cognitively healthy elders. Arch. Neurol. 55, 395–401. http://dx.doi.org/10.1001/archneur.55.3.395.

Schöll, M., Lockhart, S.N., Schonhaut, D.R., Schwimmer, H.D., Rabinovici, G.D., Correspondence, W.J.J., Schö Ll, M., O 'neil, J.P., Janabi, M., Ossenkoppele, R., Baker, S.L., Vogel, J.W., Faria, J., Jagust, W.J., 2016. PET imaging of tau deposition in the aging human brain. Neuron 89, 971–982. http://dx.doi.org/10.1016/j.neuron.2016.01.028.

Schwarz, A.J., Yu, P., Miller, B.B., Shcherbinin, S., Dickson, J., Navitsky, M., Joshi, A.D., Devous Sr., M.D, Mintun, M.S., 2016. Regional profiles of the candidate tau PET ligand 18 F-AV-1451 recapitulate key features of Braak histopathological stages. Brain 139 (5), 1539–1550.

Sperling, R. a, Rentz, D.M., Johnson, K. a, Karlawish, J., Donohue, M., Salmon, D.P., Aisen, P., 2014. The A4 study: stopping AD before symptoms begin? Sci. Transl. Med. 6 http://dx.doi.org/10.1126/scitranslmed.3007941, 228fs13.

Sperling, R.A., Aisen, P.S., Beckett, L.A., Bennett, D.A., Craft, S., Fagan, A.M., Iwatsubo, T., Jack, C.R., Kaye, J., Montine, T.J., Park, D.C., Reiman, E.M., Rowe, C.C., Siemers, E., Stern, Y., Yaffe, K., Carrillo, M.C., Thies, B., Morrison-Bogorad, M., Wagster, M.V., Phelps, C.H., 2011. Toward defining the preclinical stages of Alzheimer's disease: recommendations from the National Institute on Aging-Alzheimer's Association workgroups on diagnostic guidelines for Alzheimer's disease. Alzheimer's Dement. 7, 280–292. http://dx.doi.org/10.1016/j.jalz.2011.03.003.

Su, Y., Blazey, T.M., Snyder, A.Z., Raichle, M.E., Marcus, D.S., Ances, B.M., Bateman, R.J., Cairns, N.J., Aldea, P., Cash, L., Christensen, J.J., Friedrichsen, K., Hornbeck, R.C., Farrar, A.M., Owen, C.J., Mayeux, R., Brickman, A.M., Klunk, W., Price, J.C., Thompson, P.M., Ghetti, B., Saykin, A.J., Sperling, R.A., Johnson, K. a., Schofield, P.R., Buckles, V., Morris, J.C., Benzinger, T.L.S., 2015. Partial volume correction in quantitative amyloid imaging. Neuroimage 107, 55–64. http://dx.doi.org/10.1016/j.neuroimage.2014.11.058.

Su, Y., D'Angelo, G.M., Vlassenko, A.G., Zhou, G., Snyder, A.Z., Marcus, D.S., Blazey, T.M., Christensen, J.J., Vora, S., Morris, J.C., Mintun, M.A., Benzinger, T.L.S., 2013. Quantitative analysis of PiB-PET with FreeSurfer ROIs. PLoS One 8. http://dx.doi.org/10.1371/journal.pone.0073377.

Sutphen, C.L., Jasielec, M.S., Shah, A.R., Macy, E.M., Xiong, C., Vlassenko, A.G., Benzinger, T.L.S., Stoops, E.E.J., Vanderstichele, H.M.J., Brix, B., Darby, H.D., Vandijck, M.L.J., Ladenson, J.H., Morris, J.C., Holtzman, D.M., Fagan, A.M., 2015. Longitudinal cerebrospinal fluid biomarker changes in preclinical Alzheimer disease during middle age. JAMA Neurol. 72, 1–14. http://dx.doi.org/10.1001/jamaneurol.2015.1285.

Villemagne, V.L., Okamura, N., 2016. Tau imaging in the study of ageing, Alzheimer's disease, and other neurodegenerative conditions. Curr. Opin. Neurobiol. 36, 43–51. http://dx.doi.org/10.1016/j.conb.2015.09.002.

Villemagne, V.L., Pike, K.E., Chételat, G., Ellis, K.A., Mulligan, R.S., Bourgeat, P., Ackermann, U., Jones, G., Szoeke, C., Salvado, O., Martins, R., O'Keefe, G., Mathis, C.A., Klunk, W.E., Ames, D., Masters, C.L., Rowe, C.C., 2011. Longitudinal assessment of Aβ and cognition in aging and Alzheimer disease. Ann. Neurol. 69, 181–192. http://dx.doi.org/10.1002/ana.22248.

Villeneuve, S., Rabinovici, G.D., Cohn-Sheehy, B.I., Madison, C., Ayakta, N., Ghosh, P.M., La Joie, R., Arthur-Bentil, S.K., Vogel, J.W., Marks, S.M., Lehmann, M., Rosen, H.J., Reed, B., Olichney, J., Boxer, A.L., Miller, B.L., Borys, E., Jin, L.W., Huang, E.J., Grinberg, L.T., Decarli, C., Seeley, W.W., Jagust, W., 2015. Existing Pittsburgh Compound-B positron emission tomography thresholds are too high: statistical and pathological evaluation. Brain 138, 2020–2033. http://dx.doi.org/10.1093/brain/awv112.

Wang, L., Benzinger, T.L., Su, Y., Christensen, J., Friedrichsen, K., Aldea, P., McConathy, J., Cairns, N.J., Fagan, A.M., Morris, J.C., Ances, B.M., 2016. Evaluation of tau imaging in staging Alzheimer disease and revealing interactions between β-amyloid and tauopathy. JAMA Neurol. 63110, 1–8. http://dx.doi.org/10.1001/jamaneurol.2016.2078.

Wechsler, D., 1987. Manual for Wechsler Memory Scale - Revised. The Psychological Corporation doi:PCA-Converted #56.

Witten, D.M., Tibshirani, R., 2010. A framework for feature selection. Am. Stat. 105, 713–726. http://dx.doi.org/10.1198/jasa.2010.tm09415.A.